Sedimentary Geology 325 (2015) 106–118

Contents lists available at ScienceDirect

Sedimentary Geology

journal homepage: www.elsevier.com/locate/sedgeo

Deformed microbial mat structures in a semiarid temperate coastal setting

Diana G. Cuadrado [a,b,c,*], Jerónimo Pan [c,d], Eduardo A. Gómez [a,c,e], Lucía Maisano [a,c]

[a] Instituto Argentino de Oceanografía (IADO), CONICET, Florida 5000, 8000 Bahía Blanca, Buenos Aires, Argentina
[b] Depto. de Geología, Universidad Nacional del Sur, San Juan 670, 8000 Bahía Blanca, Buenos Aires, Argentina
[c] Consejo Nacional de Investigaciones Científicas y Técnicas (CONICET), Buenos Aires, Argentina
[d] Instituto de Investigaciones Marinas y Costeras (IIMyC), CONICET/Universidad Nacional de Mar del Plata, 7600 Mar del Plata, Buenos Aires, Argentina
[e] Universidad Tecnológica Nacional. Fac. Regional Bahía Blanca, 11 de Abril 378, 8000 Bahía Blanca, Buenos Aires, Argentina

ARTICLE INFO

Article history:
Received 19 February 2015
Received in revised form 2 June 2015
Accepted 3 June 2015
Available online 12 June 2015

Editor: B. Jones

Keywords:
Roll-up microbial structures
Fold microbial structures
Filamentous cyanobacteria
Tidal currents
Microbially induced mineral precipitation
SW Atlantic Ocean

ABSTRACT

This study focuses on sedimentary structures formed by microbial consortia, in a particular coastal setting, an ancient tidal channel, separated from the ocean by a sandy spit and connected by a blind tidal channel at the opposite end. Most studies in modern and ancient environments consider water movement as the triggering mechanism acting in the formation and deformation of sedimentary structures. As such, the paper documents the presence of several microbial structures such as shrinkage cracks, flip-over mats, microbial chips, and multidirectional ripples which are related to tidal processes, while bulges and gas domes structures are formed after occasional inundation events. However, the more conspicuous structures covering a great area at the study site are folds and roll-ups, the product of deformation of microbially induced structures by the action of sporadic spring-tidal currents due to strong winds. Therefore, the objective of this research is to document modern sedimentary structures in a coastal area and to provide a mechanistic explanation for their formation, based on the interplaying effects of the moisture variation and high shear stress. Also, several microbial sedimentary structures are distinguished throughout vertical sediment cores, such as microbial chips, detached mat, sponge fabrics, tears, and concentric structures, which are identified in a sedimentary profile. Through the recognition and interpretation of modern sedimentary deformation structures, this study contributes empirical tools for the reconstruction of analogous paleoenvironments in fossil studies.

1. Introduction

Microbial mats consist of consortia of prokaryotic and eukaryotic microorganisms that colonize the uppermost sediments in coastal environments altering sedimentary processes and their physicochemical properties. Thus, they have been termed a biogeomorphological force in sediments (Stal, 2010). There are two important keystones that need to be emphasized regarding the process of sediment colonization by microorganism: cohesion and geochemical variations. For cohesion, the biostabilization (*sensu* Paterson, 1994) is achieved mostly through the presence of filamentous cyanobacteria and benthic mobile diatoms in the sedimentary surface. The first ones entangle particles, and most of the motile benthic microorganisms present in the surface are embedded in highly adhesive mucilages, collectively known as EPS (extracellular polymeric substances, Decho, 1990). Consequently, the characteristics of sediments are altered, thus increasing the erosive critical threshold in aquatic environments under unidirectional currents (Hagadorn and McDowell, 2012); tidal currents (Noffke, 2010), and even wave-shear stress (Cuadrado et al., 2014).

On the other hand, the various metabolic activities of microbes alter the local geochemical and physicochemical conditions of sedimentary systems (Glunk et al., 2011), so microbial mats promote the precipitation or dissolution of some minerals. As the microbial mat has a high percent of organic matter which is rarely preserved in the fossil record, the associated mineralization provides the required lithification for preservation of microbial structures and activities. An indirect evidence of an original presence of microbial mats are the microbially induced sedimentary structures (i.e., MISS after Noffke et al., 2001a), which can be recognized in the sedimentary record. In that sense, Schieber (2004) has classified different features found in sandstones and mudstones considering steps ranging from the mat growth to the final stages of diagenesis with the destruction of organic matter and mineral precipitation. This author included the formation of polygonal cracks, roll-up, and flip-over structures within the processes involving physical mat destruction in sandstones.

The recognition of microbial mats in modern environments has gathered special relevance in recent years with regards to the

* Corresponding author at: Instituto Argentino de Oceanografía (IADO). CONICET. Florida 5000. 8000 Bahía Blanca, Buenos Aires, Argentina.
E-mail addresses: cuadrado@criba.edu.ar (D.G. Cuadrado), jeronimopan@gmail.com (J. Pan), gmgomez@criba.edu.ar (E.A. Gómez), lucia_maisano@hotmail.com (L. Maisano).

http://dx.doi.org/10.1016/j.sedgeo.2015.06.001
0037-0738/

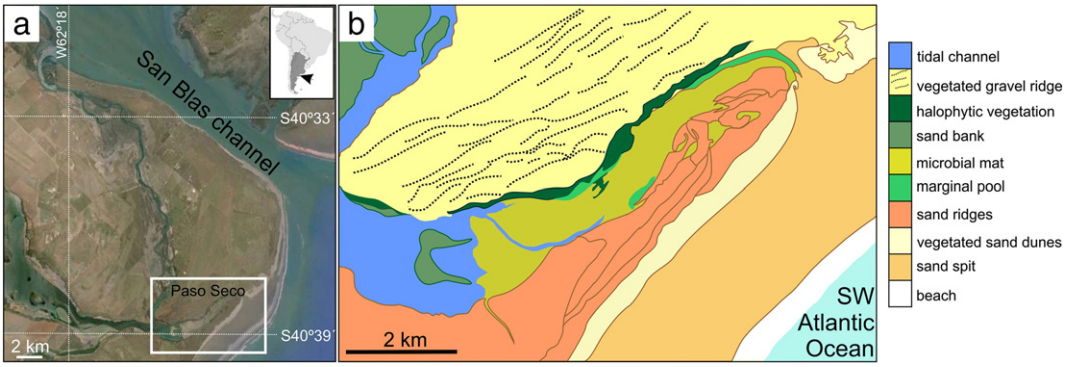

Fig. 1. Study area. (a) Location of the study area in southern Buenos Aires province, Argentina. The inset shows the location of the geomorphologic map. (b) Geomorphologic map showing the coastal plain separated from the sea by a sand spit and connected by a tidal channel to the E.

interpretation of the processes involved in the formation of sedimentary mat structures. Accordingly, recent studies carried out on the Southern Hemisphere since a few years ago (Cuadrado et al., 2012, 2013; Pan et al., 2013a) have recognized typical structures in an estuarine environment in Argentina, where tidal processes are the most important. Similarly, in modern coastal sabkhas, many studies identified sedimentary structures induced by microbial mats being related to marine processes (Gerdes et al., 2000a,b, 2008; Noffke, 2010; Aref et al., 2014 among others), and several studies recognized similar structures in the rock record (Schieber, 1999; Eriksson et al., 2000; Noffke and Awramik, 2013) and also their similarity with analogs of Martian rocks (Barbieri et al., 2006; Stivaletta et al., 2009; Noffke and Awramik, 2013).

Most works in both modern and ancient environments consider water movement as the triggering mechanisms for the deformation of sedimentary mat structures. However, the recognition of the precise physical processes behind fossil mat structures still remains a challenge, since a number of physical processes such as those dominated by currents and wind may produce similar signatures in rocks. For example, a recent study on a coastal sabkha tidal flat carried out in Tunisia (Bouougri and Porada, 2012) introduced the role of strong winds as the main process yielding mat deformation structures. The present research documents deformed sedimentary mat structures in a coastal area that seldom gets flooded by seawater inundation, and where strong winds also prevail. We also identify microbial structures in a vertical sedimentary profile in an attempt to contribute tools for the interpretation of microbial signatures in siliciclastic rocks and their associated processes of formation. This study in a modern setting promotes the recognition of analogous structures in fossil records and the consequent inference in paleoenvironmental research.

2. Methods and study area

This paper is based on *in situ* observation, and field and laboratory studies corresponding to six campaigns carried out in the temperate coastal flood plain environment at Paso Seco, Argentina (40°33′S; 62°14′W, Fig. 1). These campaigns took place in January 2013 (mid Austral summer), October 2013 (mid Austral spring), March 2014 (early Austral autumn), October 2014, December 2014 (late Austral spring), and April 2015. The campaign carried out in March 2014 was performed 1 day after a heavy rainfall, and the one in April 2015 took place coinciding with extraordinary spring tides augmented by strong winds.

The tidal amplitude was measured at spring tide with two HOBO water level loggers (model U20) to identify the tidal mitigation along the tidal channel. The conductivity and temperature of water were measured in the field with a Hanna HI9033 conductivity probe. Cylindrical sediment cores (inner diameter = 8.5 cm; height = 20 cm) were taken from the flats colonized by microbial mats and were cut longitudinally to identify microbially induced sedimentary structures. Sand samples were observed under a Nikon SMZ 1500 optical microscope

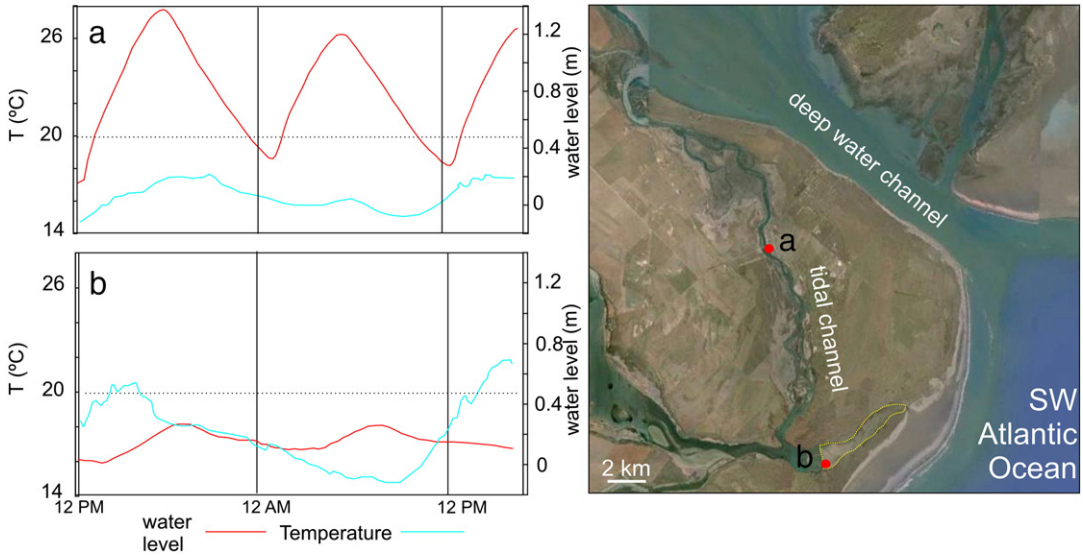

Fig. 2. Tidal range measured at two sites (a and b) along the course of the tidal channel showing their position on a satellite image on the right, where the study area is highlighted by a yellow line.

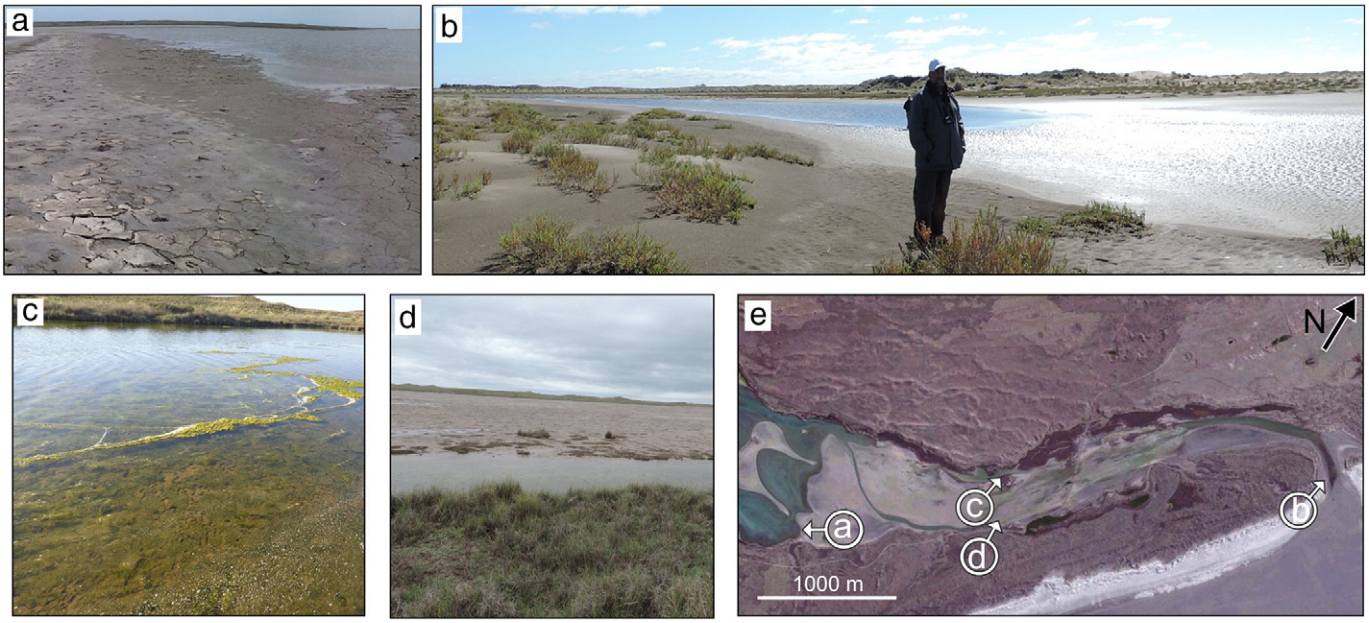

Fig. 3. Photographs illustrating the boundaries of the study area. (a) Western side where the tidal channel ends. The site is characterized by shrinkage cracks due to frequent inundation by tides. (b) Eastern side with the presence of a temporary pool near the sand spit; this is the ancient tidal channel. (c) Northern side where a marginal pool is bedded by mat pinnacles. (d) Southern side showing a narrow marginal tidal creek which ends at the point where the photograph was taken. (e) Location of the photographs on the study area. Arrows indicate the angle from which each photograph was taken.

to determine the mineralogical composition, and the grain sediment distribution was determined by standard sieving techniques.

Microbial consortia were studied from three methodological perspectives: traditional microscopic analysis, scanning electron microscopy (SEM; model JEOL35 CF 8), and community fingerprinting through molecular biology techniques. Accordingly, sampling was consistently done during daytime hours and a discrete number of microbial mat and surface sediment samples were taken for quali-quantitative light microscopy, SEM, and denaturing gradient gel electrophoresis (DGGE) analyses.

The study area, Paso Seco, is located in northern Patagonia (South America, Argentina) (Fig. 1). According to the climatic classification of Argentina proposed by Iglesias (1981), Paso Seco is located within the subdivision called "semiarid temperate of the Meseta" (see Fig. 4 and 5 in Tonni et al., 1999). This climate has an average annual rainfall < 300 mm and the potential evapotranspiration commonly exceeds precipitation (Ferrelli et al., 2012). In spite of its mid latitude and temperate condition, aridity is strong enough in the study area to limit vegetation development (see Fig. 2 in Clapperton, 1993), allowing the formation of a saline system similar to those on the coasts of northern Africa, the Arabian Peninsula, and western Asia (see Fig. 1 in Yechieli and Wood, 2002), and also similar sedimentary structures. Differences between summer and winter are relatively moderate, rather than extreme hot or cold, due to the proximity of the SW Atlantic Ocean. Rainfall is characterized by the large space–time variation, typically of semiarid regions. An important factor to take into account is the prevailing and strong winds from NE quadrant, averaging 35–38 km h^{-1} with frequent gusts up to 100 km h^{-1} (Beigt et al., 2011).

Geomorphologically, the study area comprises a large closed basin (about 2.5 × 0.3 km) colonized by microbial mats, located at a distance exceeding 1.8 km from the coastline of the SW Atlantic Ocean (Fig. 1). Previous studies have stated that this area constituted the remnants of an ancient tidal channel, which was choked by a sand spit that interrupted the outflow of the channel some 100 years ago (Espinosa and Isla, 2011). However, our records during a recent campaign showed that the area is seldom flooded during particular occasions, i.e., when very strong winds combine with the effect of the spring tide to push the seawater through a ridge-runnel channel in the sand spit to enter the water into the basin.

The blind tidal channel, that is located on the W-SW extreme of the study area, initiates in the San Blas channel at the N (Fig. 1b). The tidal amplitude was measured at two points in this tidal channel during a spring tide with HOBO water level loggers, in the mid-section of the total length and at the end of the channel (Fig. 2). While the tidal range was 1.20 m in the mid-section of the channel, it was 0.27 m at the end. Thus, such attenuation on the tide leads to a microtidal classification for the western extreme of study area inundating only tens of meters over the tidal flat (Fig. 3a). The water of the tidal channel has a salinity of 35.9‰. The northern boundary of the basin is formed by vegetated gravel ridges and bordered by halophytic vegetation, where a string of isolated pools of various dimensions (in terms of surface area and depth) are present (Fig. 3b, c). The water of these pools has a salinity ~ 25‰ and pH = 8.8 and they are most likely replenished by rain water coming from the adjacent gravel ridges. On the other hand, the southern boundary is shaped by vegetated sand ridges constituting a sand spit (Fig. 3d).

It is important to mention that the sandy sediments in the area surroundings the study zone are ferroan-titaniferous (Angelelli and Chaar, 1964; Angelelli et al., 1967). The mineralogy of the sand of Paso Seco revealed the presence of piroxen and magnetite between feldspars and quartz. The sand is mainly fine and well sorted, probably indicating aeolian sediment transport.

Fig. 4. Microbially induced sedimentary structures related to the tidal channel. (a) Desiccation cracks due to solar radiation after tidal inundation; these are simple, triradiate, and curved.(b) Flipped-over edges. Edge of mats inverted locally due to water action. Some have initial curling due to desiccation. They are flipped over in the direction of the tidal current. Note the wet underlying sediment. (c) Erosional stage at the shoreline of the tidal channel. Some coherent mat hangs over the small cliff (arrow). Vegetation of the glasswort *Sarcocornia ambigua* is spread over the upper level, evidencing a small cliff due to tidal inundation. (d) Microbial chips. Fragments of flattened microbial mat that have been broken by currents or wave action. (e) Upper level is covered by sand detritus and burrows; the vertical burrows are also seen in sediment cores (see Fig. 7b). (f) Multidirectional ripples. Two generation of ripples displayed in the same tidal surface with an angle due to different orientation of wind-waves.

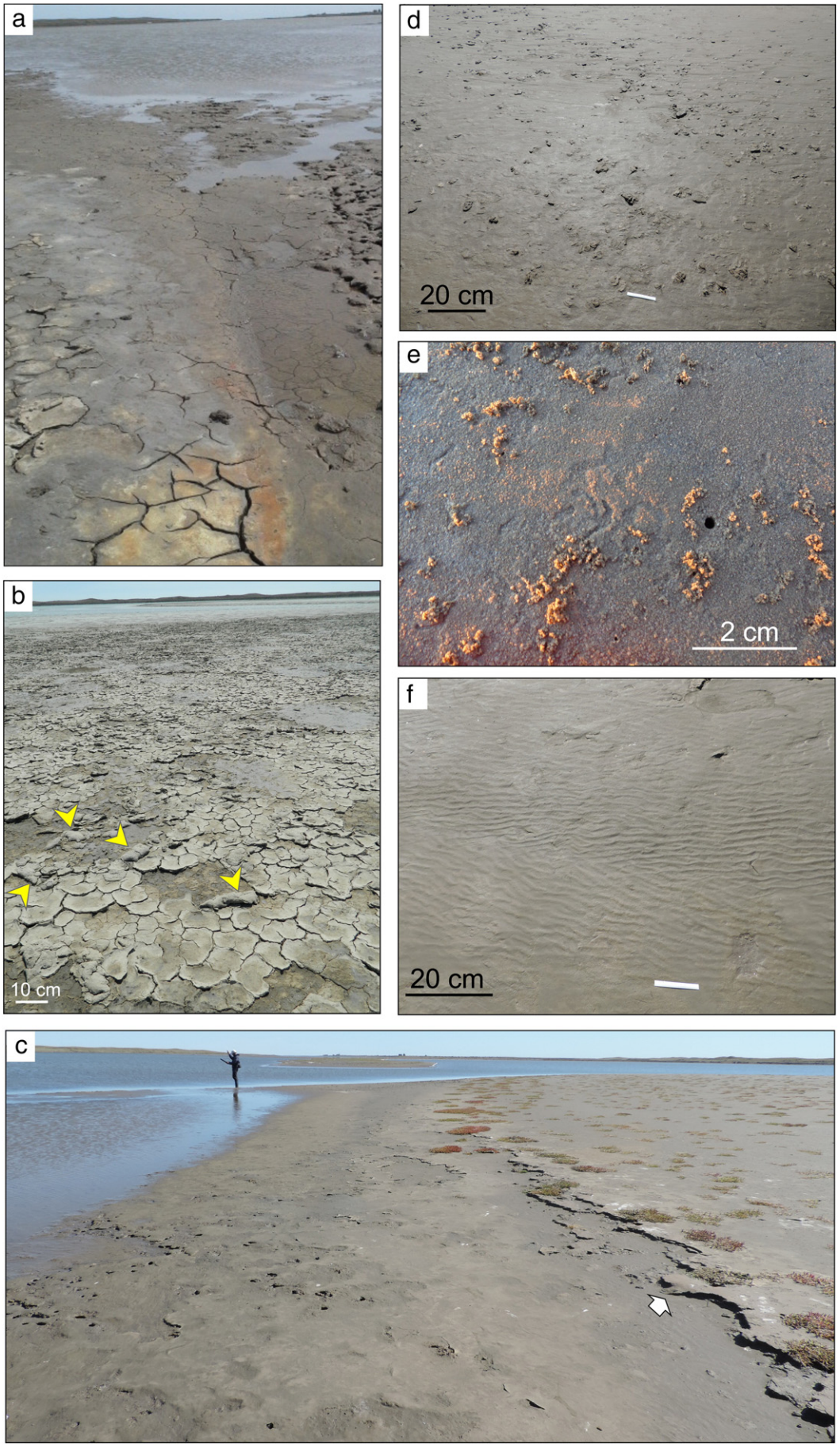
a
b
10 cm
c
d
20 cm
e
2 cm
f
20 cm

3. Results

3.1. Sedimentary microbial structures and their spatial distribution.

The study area is flanked by gravel vegetated ridges to the north, sand spit to the south, and a tidal channel (connected to the sea in the north) to the west. Except for a vegetated patches of the cordgrass *Spartina densiflora* and the glasswort *Sarcocornia (Salicornia) ambigua*, almost all of the tidal plain is colonized by thick and coherent laminated microbial mats (see geomorphologic map, Fig. 1b). It presents a low gradient which, after episodic heavy rainfall, and when the water table ascends generates the surface water to "slide" over the mats. The basin is also rarely inundated by tides during specific conditions (spring tides in conjunction with strong winds). Different microbial mat structures have been found in the study site, which are herein typified into three categories.

3.1.1. Microbial structures type I

These structures are present mainly along the shoreline of the tidal channel, westward of the studied zone. They consist of desiccation cracks with upward curved edges, flipped-over edges structures, microbial chips, and multidirectional ripples (Fig. 4). They are present not far from the tidal channel and their generation is related to frequent flooding and desiccation events.

After high tide, the microbial mat is exposed to hot and dry conditions evaporating the water from the sediments. Therefore, linear and sinuously curved cracks open with the change in sediment moisture due to subaerial exposition (Fig. 4a). Then, desiccation cracks with a U-shape profile are formed showing a polygonal pattern of fractures with uplifted margins as a stage of evolution (Fig. 4b). The incipient curling is due to the differential (more) shrinkage of the mat in relation to the sandy substrate underneath. Some of them reached an upturned margin up to 90°. The crack network behaves as weakness lines under higher dynamic conditions and flipped-over mat edges are formed; when this happens, they make a complete inversion of mat edge, which points to a non-elastic behavior, and they may indicate the direction of flood or ebb currents. They are also isolated features that expose the underlying wet substrate (Fig. 4b).

The occurrence of high energy events is also supported by the presence of mat chips scattered randomly across the tidal flat near the channel but at a higher level (Fig. 4c). They are made by muddy sediment and have sharp edges inferring minimal transport (Fig. 4d). This surface is also colonized by the glasswort *S. ambigua* confirming that the surface is inundated in infrequent episodes. On the same high level, sediment detritus were found on a large extension (Fig. 4e) made by insects (Coleoptera: Polyphaga: Hydrophilidae; A. Toledo, pers. comm.) that make vertical burrows crossing the mats. Also, this higher surface acts as a step for the channel inundation protected by the microbial mat colonization. Below this level, where periodic tidal inundation occurs, multidirectional ripples are present with two different orientations (Fig. 4f). After the generation of one sequence of ripple marks, the mat colonization stabilizes the surface. Later, during another event of inundation, the ripples with other orientation, probably due to different wind direction, were stabilized by another instance of mat growth.

3.1.2. Microbial structures type II

This classification type includes overgrowth patterns which are common in sabkha environments (Gerdes, 2010), and it also corresponds to the mat growth process in the classification defined by Schieber (2004). Microbial structures are found mainly near the marginal pools where the water table is closed to the surface. The salinity of groundwater ranges between 44‰ and 98‰. Some of these structures have round crested bulges in irregular shape, and others present more advanced desiccation and cracks at peaks of domal feature (Fig. 5a–c). Dark zones on the surface (Fig. 5c) represent sites of uprising groundwater and induced microbial activity (Eriksson et al., 2010).

3.1.3. Microbial structures type III

This classification type includes microbial mat deformation structures (MDS) defined by Bouougri and Porada (2012). In the present study, they occur at the central part of the colonized flat and have no contact whatever with permanent water from neither the tidal channel nor the marginal pools. These structures are folds and roll-ups shaped by strong forces. They are made up by a very thick microbial mat (>1 cm) which is loosely attached to the underlying sedimentary layers. Stages in the development of these folds comprise firstly a tear formed due to solar radiation (that acts as a weakness line) and then, under high shear stress acting on the flexible and wet mat surface, folds are formed over the slippery substrate (Fig. 5d). Under higher shear stress, roll-ups might be made with several involutions in different directions and moved along the surface over a distance of several meters as a piece of cloth or rug (Fig. 5e). Most of these flattened roll-ups are developed in the same direction of the longitudinal axis of the area. Flipped-over edges were also found, and probably this is the first step of roll-up structures. On the other hand, microbial recolonization of the mats was observed (Fig. 5f).

Another frequent feature in the area that deserves attention are rather small ponds (~0.5 m^2, 5 cm deep) with "milky water" (as was called by Shinn and Kendall, 2011) that were found during the early spring. The hypersaturated water (S = 110‰; T° = 24.4 °C) is white in color and occurs in small shallow depressions over the low-permeable microbial mat (Fig. 6a). This water is transformed into evaporites during summer (Fig. 6b), and the whiting, once evaporated, has a great amount of halite and also the presence of needles of aragonite (8 μm in size).

3.2. Vertical cores

Sections of bedded sequences show the progression of microbial mat growth interlaying mainly with sand (Fig. 7). The microbial mat grows forming biolaminites (Gerdes et al., 2000b), light and dark thin layers. They are separated by wide layers of sand which reach up to 4 cm in thickness, reflecting an energy increase in the environment. Also, some small gravel sediments can be observed amongst sand (Fig. 7b). Brownish laminae can be noted indicating high amounts of organic matter and also iron oxides. Mat laminae are flat but they occasionally bend in a wavy-crinkly lamination fashion, mainly when they are comprised by fine cohesive sediment. Reducing conditions are also seen as dark zones without any special control (Fig. 7a) which avoid seeing the fine lamination. Mat laminae are disposed mainly horizontally, but sometimes buckled layers are recognized (Fig. 7c).

3.3. Microbial consortia

The consortia of prokaryotic and eukaryotic microorganisms that colonize surface sediments exert a control over the construction, morphology and behavior of sedimentary structures to a great extent, in addition to modifying the physicochemistry of sediments and creating micro-habitats. In this environment, the dominant mat-constructing microbial group appears to be non-heterocystous, trichome-forming cyanobacteria (order Oscillatoriales); while a substantial proportion of the total biomass is also contributed by benthic diatoms.

The microscopic analysis of surface sediment cores (uppermost 2–8 mm) taken in early spring 2013 and late summer 2014 evidenced a significant environmental/spatial heterogeneity with respect to the cyanobacteria and diatom consortia that dominated surface sediments. Most sedimentary structures and sampling sites presented consortia well represented by the three above-mentioned groups (i.e., pennate and centric diatoms, filamentous cyanobacteria). Without exception,

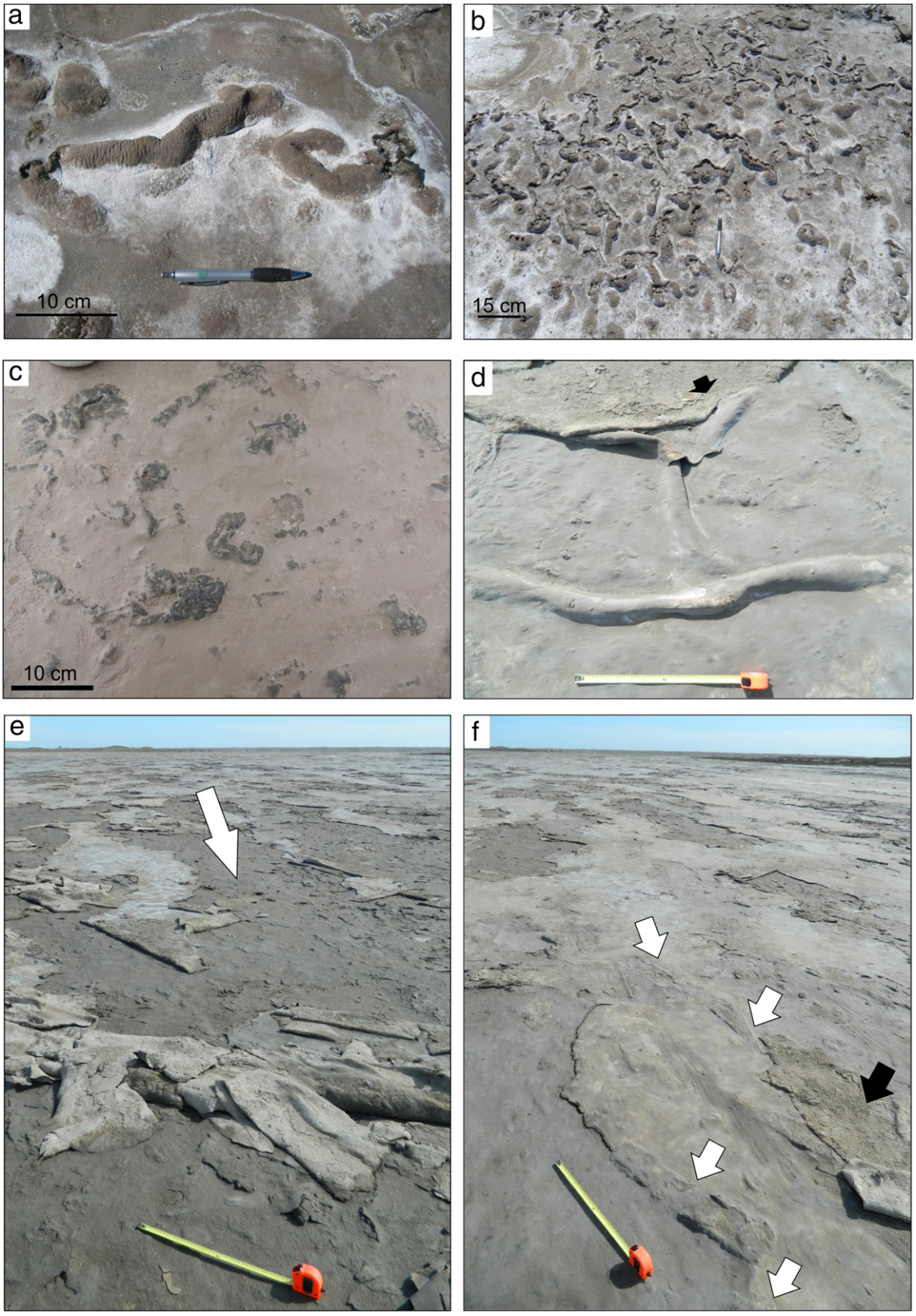

Fig. 5. Microbially induced sedimentary structures type II and III. (a) Elongated bulges with gas entrapped under the mat. Efflorescent halite is formed over the mat. (b) Desiccation at the peak of the irregular bulges due to radiation. Halite is also precipitated. (c) Dark zones at the top of bulges evidence difference in moisture content of the sediments. (d) Two folds formed by a detached mat from the underlying substrate by wind. The two perpendicular directions of folds reveal the movement of the detached mat under high wind-shear stress. Note the start of detachment (arrow). (e) Roll-up structures of the detached mat initiated from shrinkage cracks and mat tears. Note the amount of microbial mat with several involutions at the foreground of the photograph. In spite of the different directions of the roll-ups, the higher frequency of tears with a single direction allows to infer the dominant wind direction (white arrow). (f) Flipped-over mats showing microbial recolonization (arrows). There is a new roll-up exhibiting the underlying sediment (black arrow). Note the different colors of colonized sediments indicating distinct stages of colonization. Metric tape is 50 cm.

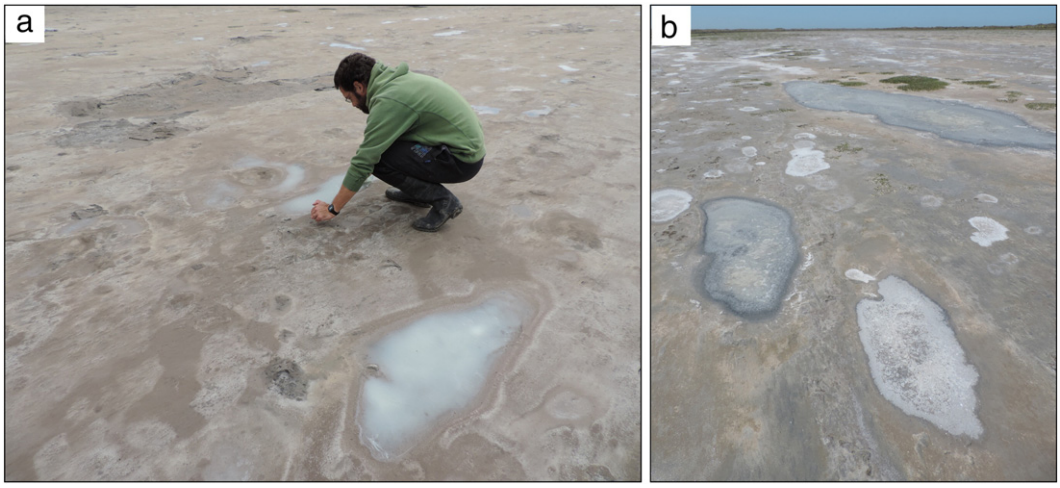

Fig. 6. Presence of "milky water" over the colonized flat. (a) Small very shallow ponds (<5 cm deep) formed with whitings, carbonates in suspension, over the large microbial mats after a rainfall (in spring). (b) Precipitation of evaporites by solar heating, mainly halite. Note the different color in deeper ponds (5 cm depth) where patches with milky water still remain (right and upper side).

pennate diatoms were consistently more abundant than centrics. Naviculoid genera such as *Navicula* sp., *Diploneis* sp., *Gyrosigma* sp., and *Nitzschia* sp. were among the representatives of the former while centric representatives comprised genera such as *Melosira* sp. and *Podosira* sp. Pennate diatoms increased their abundance near the marginal ponds (see Fig. 3c).

When present, filamentous cyanobacteria (i.e., representatives of the order Oscillatoriales, such as *Microcoleus chthonoplastes* and *Symploca* sp.; Fig. 8) made up for the larger portion of the total biomass of the microbial consortium, even if pennate diatoms contributed a significant proportion; this is due to the trichomous nature of the dominant cyanobacteria which were found at an average densities of up to ~ $376 \pm 15 \times 10^3$ trichomes cm^{-3} (Fig. 8a). These non-heterocystous filamentous cyanobacteria grow conspicuously in the upper mm of microbial mats and on the undersides of upraised cracks, in order to find the optimal light intensity for photosynthesis. A highly coherent structure is produced by the interwoven filaments (trichomes) of these cyanobacteria (Fig. 8a, c), providing a dense and coherent fabric for the binding of sedimentary particles and giving a remarkable external leathery appearance to the microbial mat, especially apparent in physically deformed structures. A striking feature of these thick mats is the resulting high elastic behavior, product of the cohesiveness (Video 1 in Appendix A). In turn, this sets the necessary conditions for a torn mat to exhibit flexible deformation under high shear stress.

Furthermore, the presence of free-living bacteria and archaea DNA was corroborated in all water ($n = 5$) and most sediment samples ($n = 6$, out of 7) (data not shown). These preliminary results are currently being further analyzed with molecular biology techniques in order to determine the taxonomic groups to which these microorganisms belong.

4. Discussion

4.1. Microbial structures

Three spatially segregated types of structures generated and governed by different processes were determined. Solar irradiance is one of the parameters that affect the colonized sediments thus conditioning the formation of some of the structures in this coastal environment. The intertidal zone, near the tidal channel westward of the study area, is characterized by periodic inundation by seawater (either fortnightly during spring tides, monthly or eventually during storms). Here, it is frequent the formation of shrinkage cracks, which originate after the subaerial exposition and desiccation of the microbial mat during a dry period, while the sandy bottom remains flat (Fig. 4a). They can be stripped under wet conditions leaving the underlying sediments exposed (Fig. 4b). The microbial cracks may begin as incipient tears and may evolve into triradiate cracks and polygonal networks, sometimes developing curled borders. The mat chips, not rounded and resembling mudclasts, are found not far from the coastline of the tidal channel and are related to erosional events by high energy tidal currents. These type I microbial structures are similar to those found in the supratidal zone of estuarine environments, as the temperate Bahía Blanca estuary (Cuadrado et al., 2011, 2014; Pan et al., 2013b) and in different estuarine areas of the world (e.g., Mellum Island, thoroughly described by Noffke et al., 2001a), lake environments (e.g., the Egyptian coast studied by Taher and Abdel-Motelib, 2014), and coastal sabkhas (e.g., the Tunisian coast researched by Noffke et al., 2001b). Eriksson et al. (2007) named these structures as mat-destruction features and found them in sandstones in the rock record.

Microbial structures type II, such as bulges structures, are present near the ponds where the water table keeps close to the surface. Probably they are dominated by coccoid cyanobacteria where inundation is rare (Bouougri et al., 2007; Bouougri and Porada, 2012). Their localized growth and cell division lead to pustular or cauliflower-like surface structures. Dark areas at the top of the bulges receive a differential moisture supply, indicating the rising up of groundwater from the sediment below, a common process in sabkha environments (e.g., from the Tunisian coast, Gerdes et al., 2000a, 2008; Eriksson et al., 2010). Both types, I and II, follow some of the principles pointed by Eriksson et al. (2010) with regards to the frequency and duration of inundation and the relative position of groundwater.

The most significant microbial structures observed in this coastal environment were those classified as type III, i.e., deformed microbial mats in the shape of folds and roll-ups. The thickness of the mat is at least 1 cm and the genetic processes are initiated when it is desiccated and cracked due to solar irradiance

Fig. 7. Vertical sediment cores. (a) (b) (c) Photographs of cores showing different sedimentary structures. Note the reddish-brown color in (a) due to iron oxides and the coarser sand under the detached mat. The separation between microbial mats was refilled by sand in (b) (black arrow) and coarser sand and small gravels were immediately over the microbial mat where the tear is present, indicating the increase in wind-energy level. See text for details. (c) Involuted microbial layers resembling crenulation, bulges, or folds, similarly that were found over the surface. (d) (e) (f) Schematic representation of cores. dm: detached mat. sf: sponge fabrics. t: tear. mc: microbial chips. c: involuted structure.

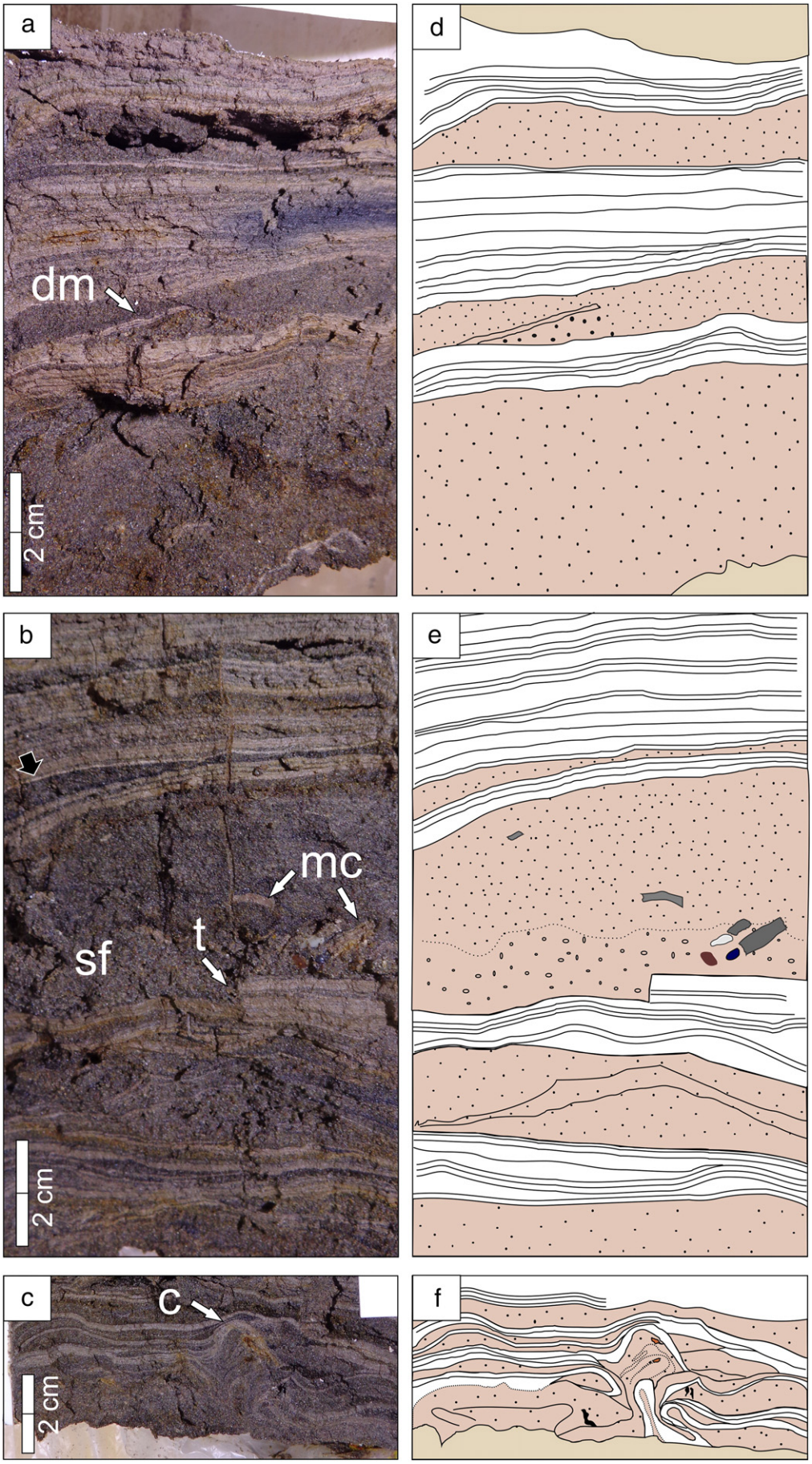
a
dm
2 cm
d
b
mc
t
sf
2 cm
e
c
c
2 cm
f

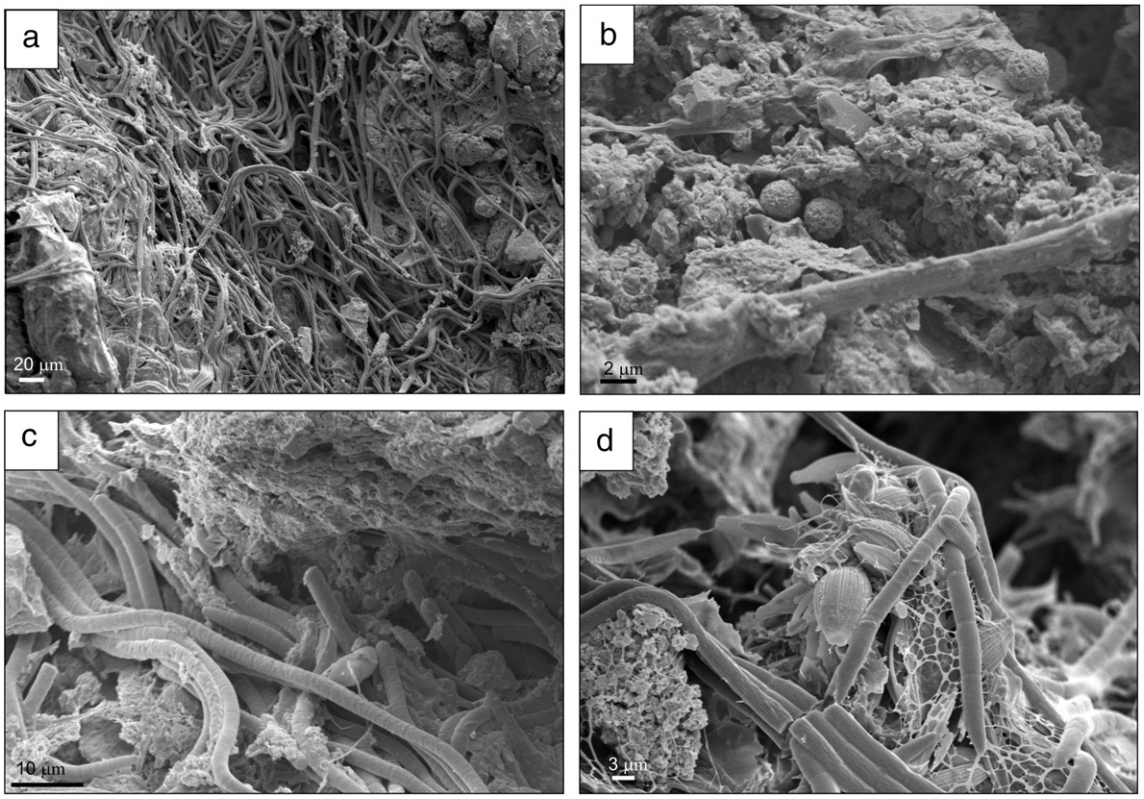

Fig. 8. Scanning electron microscopy (SEM) micrographs of microorganisms and traits of their metabolic products, found on surface sediments at Paso Seco. (a) A mesh-like arrangement with random orientation of cyanobacteria trichomes of the genus *Symploca* (Oscillatoriales). (b) Agglutinates of cells, mineral crystals, and debris, bound by exopolymeric substances (EPS). (c) Cyanobacterial trichomes at a higher magnification. (d) Pennate diatom frustules interwoven with cyanobacteria trichomes and thick EPS threads.

(Fig. 9a,b). These cracks represent lines of weakness where tears might be formed. Under this condition, the microbial mats aspect is rather rigid and leathery. However, after sporadic seawater inundation during spring tides or heavy rainfall, the water is retained over the microbial mats during several hours and they turn elastic and flexible (Video 1 in Appendix A). In the case of tidal currents, during flood and ebb, the high shear stress imparted to the wet mat makes it sweep over the subsurface forming crumpled structures, folds, and buckles (Fig. 9c). It is worth mentioning that this wide zone colonized by microbial mat is rarely affected by seawater, circumstance that only happens under special conditions. A recent observation on April 2015 campaign showed that inundation of the area by seawater can occur when strong NE winds blow during several days in conjunction with spring tide and with water-saturated substratum after rainy days. The subsequent action of currents over the thick microbial mats forms folds and several roll-ups with their axis perpendicular to the longitudinal direction of the area (Fig. 10).

Also, observations carried out during the inundation of microbial mats after rainfall showed the formation of large gas domes (about 20 cm in diameter) appearing out of the water level (Fig. 9d, Video 2 in Appendix A). Gas domes develop due to microbial gassing (either O_2 production through photosynthesis, CO_2 production due to bacterial activity and organic matter decay), underneath EPS-rich microbial mats constructed by filamentous cyanobacteria, which avoid much of the fluid exchange of gases between underlying and the water or atmosphere above (Noffke, 2010). Therefore, gas accumulates underneath the sealing flexible mat and its pressure lifts it, losing contact with the underlying substrate and generating a hollow cavity. After dry conditions, the microbial mat maintains the separation from the underlying sediments (Video 3 in Appendix A).

4.2. Cross-section sediment profiles

In vertical cross-section of sediment cores, the presence of fine laminated microbial mats (1–2 cm in thickness) alternating with thick sandy layers (4 cm) is a common feature (Fig. 7). They resemble the microsequences mentioned by Noffke (2010), although the sequence found here begins with a microbial mat, followed by the sedimentation of heavy minerals (ferroan sediments, magnetite) and subsequent sand grains (Fig. 11). Also, small gravels (2–3 mm in size) which are common in the study area would be transported by occasional tidal currents (Fig. 7b, e). Such sequence indicates that the prevailing low energy of the environment is occasionally interrupted by significantly stronger energy events. Then, the transport velocity decreases up to rather calm conditions that allow the development of microbial mats and the sequence begins again. The sand in the core is typically composed of rounded fine to very fine grains with a sponge pore fabric (Fig. 7a), a very high porosity due to gases accumulating beneath a sealing microbial mat that indicates the relation to biostabilization (Carmona et al., 2012). The intra-sedimentary gas migrates through sandy layers and the increasing gas pressure determines the occurrence of pores (0.3–1.5 mm in size). This structure is frequently found in sandstones (Noffke et al., 2003).

Several microbial structures can be appreciated in a cross-section profile. Thus, a detached mat from the underlying sediment (dm in Fig. 7a) and a rip boundary as a sharp mat disruption edge (t in Fig. 7b) can be recognized among sand laminae. The detached mat is formed as an initial phase of shrinkage after periods of solar radiation and is filled by sand transported by wind or tidal currents. After that, a tear can be formed as a consequence of a high-energy event; moreover microbial chips can be developed and is sparsely distributed in a coarser texture matrix (sand) (mc in Fig. 7b). On the other hand, deformed microbial structures are the more outstanding structure

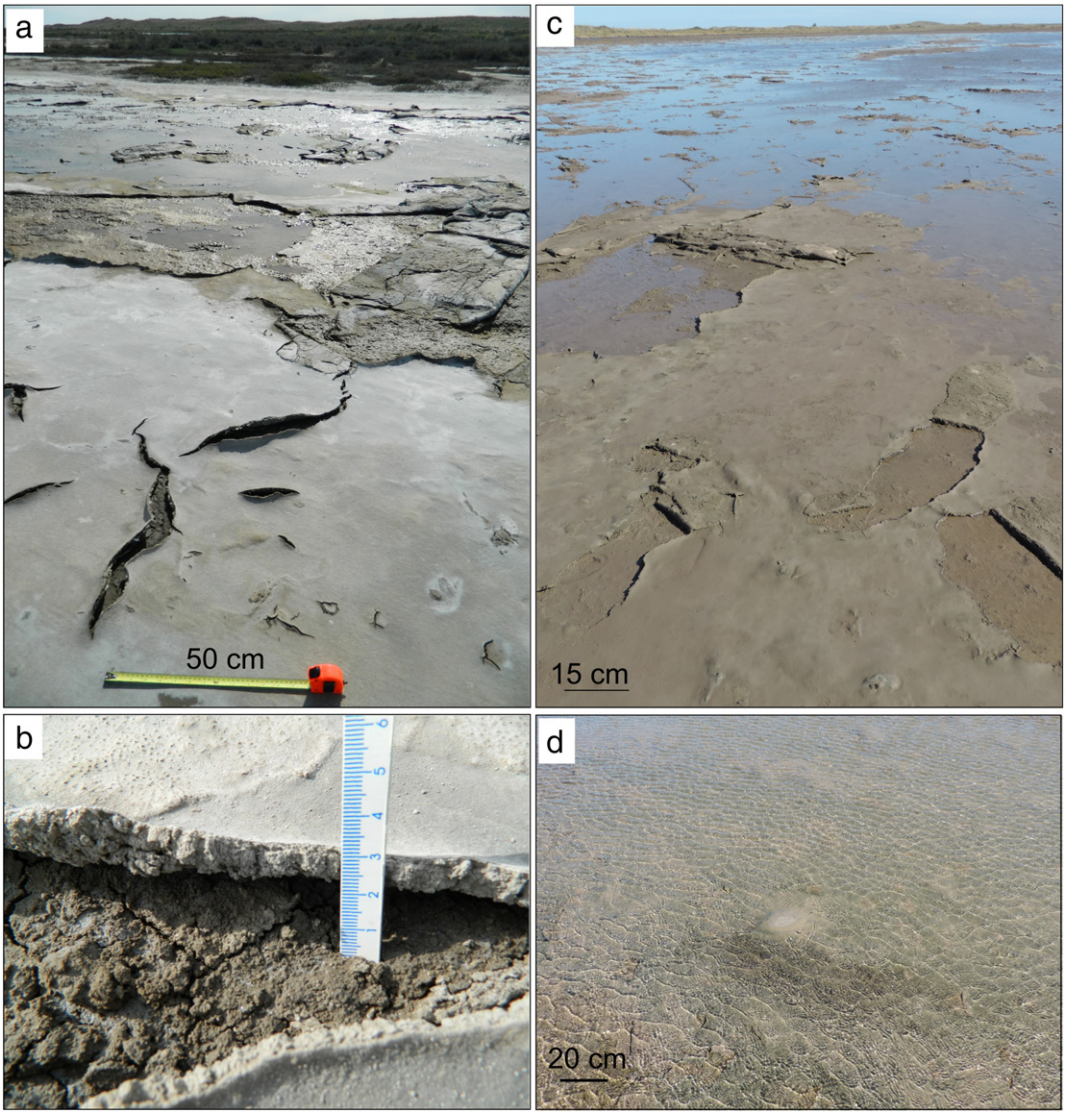

Fig. 9. (a) Initial shrinkage cracks due to solar radiation. See the wet sediment under the mat. (b) Detail of a crack over a thick mat. There are new cracks in the underlying sediment. (c) Stripped mat after a rainfall. (d) Large bubble mat, formed when the flat is inundated after a rainfall.

to be found in a sedimentary cross-section; in that sense, involuted structures (Fig. 7c) may indicate that folds and roll-up structures can be later preserved as those mentioned by Hagadorn and McDowell (2012) in ancient environments.

4.3. Biologically induced mineral precipitation

Cellular and mucilage networks created by filamentous cyanobacteria provide a remarkable cohesive strength to the sediment surface, which is more efficient than amorphous slime layers (Stal, 2000). The sheath material of the cosmopolitan mat builder *M. chthonoplastes*, a conspicuous microorganism present in the study area together with other cyanobacteria of the order Oscillatoriales, contains uronic acids. Dade et al. (1990) found a significant increase in the critical shear velocity required for the onset of erosion of sand particles when concentrations of polymeric uronic acid increased in the sand during *in situ* growth of bacteria. The results presented in this contribution demonstrated that very cohesive microbial mats, in which filamentous cyanobacteria are present, are deformed by high energy events (i.e., sporadic tidal currents).

On the other hand, the metabolic activity of the microbial community alters the geochemical environment, acting as an "alkaline engine" while EPS can also bind calcium ions and, along with bicarbonate in the system, constitutes an important factor setting the scenario for carbonate precipitation. In their study in a hypersaline lake, Dupraz et al. (2009) discuss the role of cyanobacteria in the process of $CaCO_3$ precipitation by the photosynthetic uptake of CO_2 and sulfate-reducing bacteria in the lithification of the mats. Although our study area is a siliciclastic environment, we found the presence of suspended carbonate in the form of white water patches over the microbial mats in Paso Seco during late spring. The photosynthesis activity of cyanobacteria removes CO_2 and induces the formation of $CaCO_3$ in suspension by raising the saturation state, thus causing the whiting of water in spring when evaporation rates are higher. In summer, after removal of 50% of the water in temporary ponds by evaporation, aragonite precipitates; further, when 90% of the water has been removed, halite precipitates (Libes, 1992). Accordingly, a microscopic analysis of sediment samples obtained from the evaporated white-water ponds showed the presence of needles of aragonite and cubes of halite. The photosynthetic cyanobacteria present in the study area may be fertilized by ferruginous weathering products of silicates and Fe oxides, abundant minerals in the area (Angelelli and Chaar, 1964; Angelelli et al., 1967; Fig. 11). This association of carbonates, evaporites, and siliciclastic sediments indeed needs further research in this coastal

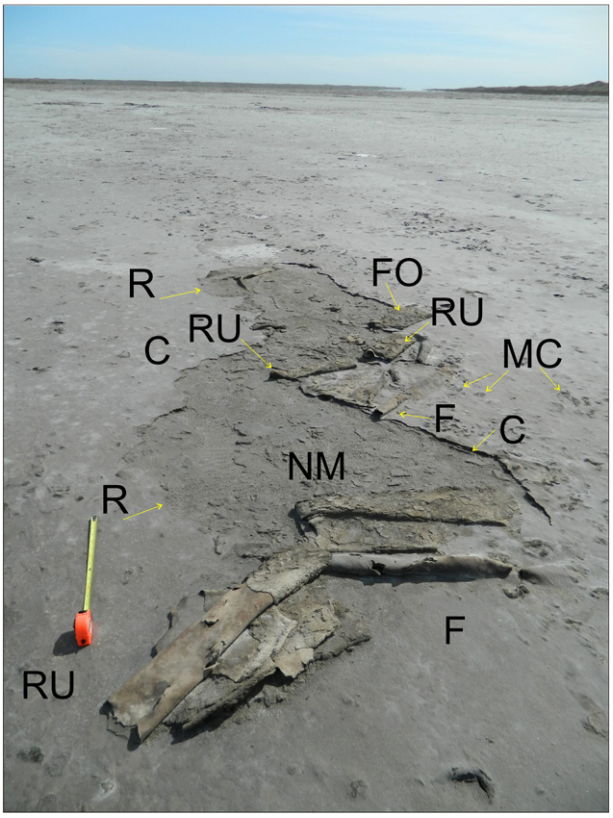

Fig. 10. Photograph showing the deformation and re-working of a thick microbial mat on the coastal plain due to wind stress and the resulting sedimentary structures, namely, C: cracks, FO: fold-over, RU: roll-up, F: fold, and NM: new mat; R: recolonization, MC: microbial chips. Metric tape is 50 cm.

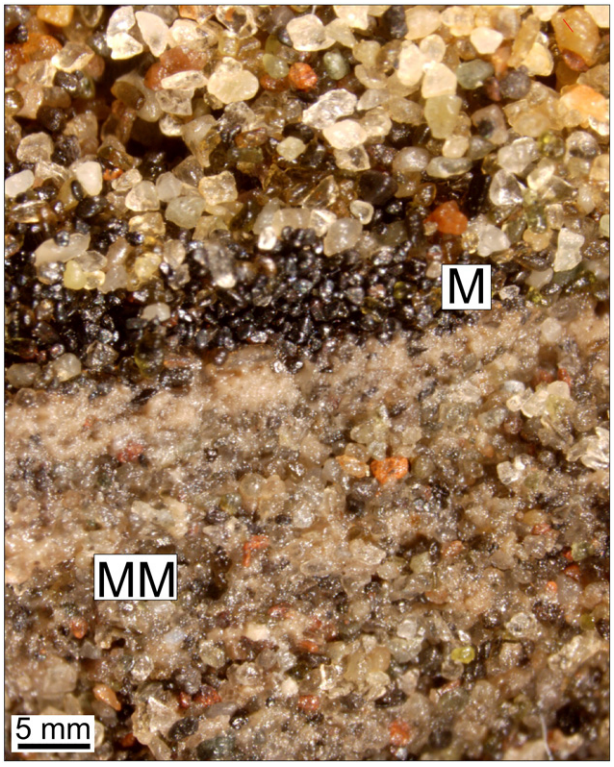

Fig. 11. Vertical profile showing the microbial mat (MM), sediment grain embedded in EPS with carbonate precipitation (light zones). Magnetite (M) overlays the microbial mat and then medium sand is present (quartz, feldspars, pyroxene). The microbial mat reflects low sedimentation, while the overlying sediments represent increased sediment transport. The sedimentation begins with heavy minerals such magnetite (M).

area, in view of recognizing microbially mediated processes such as the bacterial mediation of mineral precipitation. A recent example was presented by Swart et al. (2014), who considered the turning of water white and the formation of carbonate whitings to explain in part the building of the Great Bahama Bank, in the presence of cyanobacteria.

4.4. Hydrodynamic model

The northern marginal pool (marked as C in Fig. 3) has a salinity ~23‰, rising up to 44‰ in summer when it becomes partly dried up. This pool is flanked on its northern side by gravel ridges (Fig. 1b) that act as very permeable beds where the precipitation infiltrates to replenish the underlying phreatic aquifer and the pond itself. However, small ponds that remain over the microbial mat surface after a rainfall event or seldom tide inundation increase their salinity to 80–90‰ (up to 116‰ in summer) due to excess evaporation by high solar irradiance. Groundwater also has high salinity values, ranging from 44 to 98‰ (measured in the hollows after each core extraction). Moreover, the unconfined aquifer is under an upward hydraulic pressure which is higher where the flow of water enters to the system by rainfall than the sea level (tidal channel and seawater in this case) (Fig. 12). This hydraulic pressure is raised after rainfalls and unusual high spring tide incoming from the east, and therefore there is an uplift force with the potential to detach the microbial mats from the underlying sediments (Porada et al., 2007; Cuadrado et al., 2014). Under such conditions, the liquefied sand below the microbial mat acts as a slippery surface, and the high flexibility on wet mats affected by strong tidal current shear stress sets the scenario for the formation of mat folds, buckles, and roll-ups. Another factor such as the metabolic gassing produced during the photosynthetic activity of microorganisms and decay of buried mat material creates flexible surface domes due to trapped gases below the mat. The underlying hollows are later filled by the liquefied sediment rising up from the mat substratum. The same process occurs for the microbial fold cavities.

In this environment, where the evaporation rate is high, there is also a hydrodynamic movement of saline interstitial waters to replace the evaporative water-loss near the surface. This is an uplift force defined by Hsu and Siegenthaler (1969) as “evaporative pumping” in an arid coastal plain in contrast to capillary forces caused by surface tension in a vadose zone. This vertical hydraulic gradient is much larger in fine sediment than that in coarse sediment, if the same amount of evaporative loss is to be replaced. The movement of saline waters by evaporative pumping would explain the dark zones over the bulges, which appear in this coastal environment. Similarly, Gerdes et al. (2000b) explained these bulge-like mat expansion structures as the result from localized excessive microbial growth and biomass accretion induced by uprising groundwater stimulated by evaporation in sabkha.

Furthermore, the presence of whitings in a siliciclastic environment under a temperate climate indicates that the processes involved are similar to those occurring in arid carbonate environments. Warren (2006) stated that Holocene evaporitic carbonates are the best analogs for many Precambrian marine carbonates. So, the results from our study in this environment might provide important insights into the interpretation of the fossil record.

5. Conclusion

The coastal environment presented in this paper is isolated from the adjacent ocean by a sandy barrier, but there is a tidal channel in the opposite cardinal direction that floods only a narrow zone. Consequently,

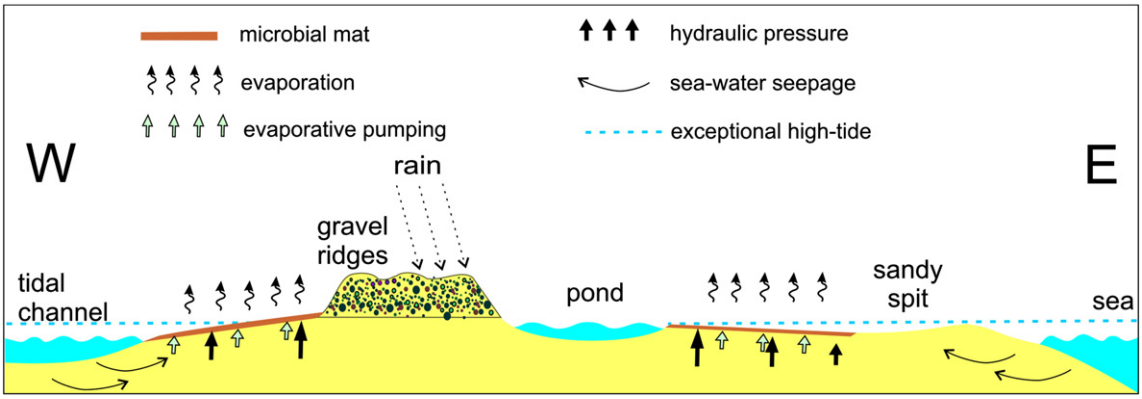

Fig. 12. Schematic model of the coastal plain at Paso Seco. The area is protected from the sea by the sand spit and receives surface water during rain events. Rainfall enters the unconfined layer at the hydraulic heads (gravel ridges) and leaves it in the sea or tidal channel. The hydraulic pressure is higher near the hydraulic heads and diminishes towards the sea level, taking into account the seepage of seawater through the sand spit. The evaporative pumping forces are caused by evaporation. The tidal channel and the ocean water are at the same mean level. This diagram emphasizes that the main factors driving water balance in the study area are rain and evaporation. However, it is important to consider the occasional inundation at specific times (i.e., the conjunction of several days of strong winds and spring tide after rainy days) when the seawater crosses the sand spit and enters the basin colonized by microbial mats. More details in the text.

some microbial sedimentary structures in this environment are related to periodic tidal inundation. These are desiccation cracks with upward curved edges, flipped-over edges, microbial chips, and multidirectional ripples. The more relevant deformed sedimentary structures are folds and roll-ups. These structures are formed as a consequence of two complementary factors, strong winds during spring tide that make the ocean waters enter the coastal basin behind the sand spit, where previous rain events had recharged the groundwater storage. The upward hydraulic pressure and tidal currents induces the mat detachment from underlying sediments after rainfall in the hinterland. The mat makes it sweep over the subsurface forming crumpled, fold, and roll-up structures.

The microbial consortia that make up the mats are dominated by filamentous non-heterocystous cyanobacteria and also by pennate and centric diatoms. Molecular signatures for bacteria and archaea have also been found. The interwoven filaments of these cyanobacteria produce a highly coherent fabric that gives a remarkable leathery appearance to the microbial mat, especially in physically deformed structures. A striking feature of these thick mats is the resulting elastic behavior, product of their cohesiveness, under high shear stress.

The microbial sedimentary structures found in the surface could also be identified in a vertical sedimentary profile. Thus, microbial chips, detached mat, sponge fabrics, tears, concentric structures that resemble folds or roll-ups are seen in sedimentary cores. The detection of these deformed-mat structures might help in the reconstruction of paleoenvironments where a couple of forces are dominant, the wind and water currents being the triggering mechanism of deformation. Accordingly, the structures and processes studied in modern environments contribute to the unraveling of depositional paleoenvironments inferred from ancient clastic rocks.

Supplementary data to this article can be found online at http://dx.doi.org/10.1016/j.sedgeo.2015.06.001.

Acknowledgments

This work was supported by grants PICT 309/12 from ANPCyT, PIP 2013 N°112 from CONICET, PGI 24/ZH20 from SECyT-UNS and PID 25/B035-UTI989 UTN. L. Maisano was supported by an Initial Fellowship from ANPCyT. D. Nercessian, M.I. Giménez (IIB/CONICET) and C. Hozbor (INIDEP) processed the samples for molecular techniques. We thank J. Spagnuolo for microscopic identification of minerals, L.A. Raniolo for his assistance in the field, C. Gutierrez Ayesta for assistance with SEM analysis, and A. Toledo for identification of coleopterans. We thank M. Aref for constructive comments on the ms.

References

Angelelli, V., Chaar, E., 1964. Las arenas de la Bahía San Blas, su investigación por minerales de hierro, titanio y zirconio (partido de Carmen de Patagones, provincia de Buenos Aires). Comisión Nacional de Energía Atómica, Buenos Aires.

Angelelli, V., Villa, J., Suriano, J.M., 1967. Los depósitos de titanio-magnetita illmenita y circón de Bahía San Blas (tramo baliza La Ballena-Faro Segunda Barranca), partido de Carmen de Patagones, provincia de Buenos Aires. Comisión Nacional de Energía Atómica, Buenos Aires.

Aref, M.A.M., Basyoni, M.H., Bachmann, G.H., 2014. Microbial and physical sedimentary structures in modern evaporitic coastal environments of Saudi Arabia and Egypt. Facies 60, 371–388.

Barbieri, R., Stivaletta, N., Marinangeli, N., Ori, G., 2006. Microbial signatures in sabkha evaporite deposits of Chott el Gharsa (Tunisia) and their astrobiological implications. Planetary and Space Science 54, 726–736.

Beigt, D., Cuadrado, D.G., Piccolo, M.C., 2011. Study of the surface water circulation in San Blas channel (Argentina) using Landsat imagery. Brazilian Journal of Oceanography 59, 241–252.

Bouougri, E.H., Porada, H., 2012. Wind-induced mat deformation structures in recent tidal flats and sabkhas of SE-Tunisia and their significance for environmental interpretation of fossil structures. Sedimentary Geology 263-264, 56–66.

Bouougri, E., Gerdes, G., Porada, H., 2007. Inherent problems of terminology: definition of terms frequently used in connection with microbial mats. In: Schieber, J., Bose, P.K., Eriksson, P.G., Banerjee, S., Sarkar, S., Altermann, W., Catuneau, O. (Eds.), Atlas of microbial mat features preserved within the clastic rock record. Elsevier, Amsterdam, pp. 145–151.

Carmona, N.B., Ponce, J.J., Wetzel, A., Bournod, C.A., Cuadrado, D.G., 2012. Microbially induced sedimentary structures in Neogene tidal flats from Argentina: paleoenvironmental, stratigraphic and taphonomic implications. Palaeogeography, Palaeoclimatology, Palaeoecology 353-355, 1–9.

Clapperton, Ch.M., 1993. Nature of environmental changes in South America at the Last Glacial Maximum. Palaeogeography, Palaeoclimatology, Palaeoecology 101, 189–208.

Cuadrado, D.G., Carmona, N.B., Bournod, C.A., 2011. Biostabilization of sediments by microbial mats in a temperate siliciclastic tidal flat, Bahia Blanca estuary (Argentina). Sedimentary Geology 237, 95–101.

Cuadrado, D.G., Carmona, N.B., Bournod, C.N., 2012. Mineral precipitation on modern siliciclastic tidal flats colonized by microbial mats. Sedimentary Geology 271-272, 58–66.

Cuadrado, D.G., Bournod, C.N., Pan, J., Carmona, N.B., 2013. Microbially-induced sedimentary structures (MISS) as record of storm action in supratidal modern estuarine setting. Sedimentary Geology 296, 1–8.

Cuadrado, D.G., Perillo, G.M.E., Vitale, A., 2014. Modern microbial mats in siliciclastic tidal flats: evolution, structure and the role of hydrodynamics. Marine Geology 352, 367–380.

Dade, B., Davis, J.D., Nichols, P.D., Nowell, A.R.M., Thistle, D., Trexler, M.B., White, D.C., 1990. Effects of bacterial exopolymer adhesion on the entrainment of sand. Geomicrobiology Journal 8, 1–16.

Decho, A.W., 1990. Microbial exopolymer secretions in ocean environments: their role(s) in food webs and marine processes. Oceanography Marine Biology Annual Review 28, 73–153.

Dupraz, C., Reid, R.P., Braissant, O., Decho, A.W., Norman, S.R., Visscher, P.T., 2009. Processes of carbonate precipitation in modern microbial mats. Earth-Science Reviews 96, 141–162.

Eriksson, P.G., Simpson, E.L., Eriksson, K.A., Bumby, A.J., Steyn, G.L., Sarkar, S., 2000. Muddy roll-up structures in siliciclastic interdune beds of the ca 1.8 Ga Waterberg Group, South Africa. Palaios 15, 177–183.

Eriksson, P.G., Porada, H., Banerjee, S., Bouougri, E.H., Sarkar, S., Bumby, A.J., 2007. Mat-destruction features. In: Schieber, J., Bose, P.K., Eriksson, P.G., Banerjee, S.,

Sarkar, S., Altermann, W., Catuneanu, O. (Eds.), Atlas of Microbial Mat Features Preserved within the Siliciclastic Rock Record. Elsevier, Amsterdam, pp. 76–105.
Eriksson, P.G., Sarkar, S., Samanta, P., Banerjee, S., Porada, H., Catuneanu, O., 2010. Paleoenvironmental context of microbial mat-related structures in siliciclastic rocks. In: Seckbach, J., Oren, A. (Eds.), Microbial Mats: Modern and Ancient Microorganisms in Stratified Systems. Springer, London-New York, pp. 73–110.
Espinosa, M., Isla, F., 2011. Diatom and sedimentary record during the mid-Holocene evolution of the San Blas estuarine complex, northern Patagonia, Argentina. Ameghiniana 48, 411–423.
Ferrelli, F., Bohn, V.Y., Piccolo, M.C., 2012. Variabilidad de la precipitación y ocurrencia de eventos secos en el sur de la provincia de Buenos Aires (Argentina). Proceeding IX Jornadas Nacionales de Geografía Física, Bahia Blanca, Argentina, pp. 15–28.
Gerdes, G., 2010. What Are Microbial Mats? In: Seckbach, J., Oren, A. (Eds.), Microbial Mats. Modern and Ancient microorganisms in Stratified Systems. Springer, Dordrecht, pp. 5–28
Gerdes, G., Krumbein, W., Noffke, N., 2000a. Evaporite microbial sediments. In: Riding, R., Awramik, S. (Eds.), Microbial sediments. Springer, Verlag, Berlin, pp. 196–208.
Gerdes, G., Klenke, T., Noffke, N., 2000b. Microbial signatures in peritidal siliciclastic sediments: a catalogue. Sedimentology 47, 279–308.
Gerdes, G., Porada, H., Bouougri, E.H., 2008. Bio-sedimentary structures evolving from the interaction of microbial mats, burrowing beetles and the physical environment of Tunisian coastal sabkhas. Senckenbergiana Maritima 38, 45–58.
Glunk, C., Dupraz, C., Braissant, O., Gallagher, K.Y.L., Verrecchia, E.P., Visscher, P.T., 2011. Microbially mediated carbonate precipitation in a hypersaline lake, Big Pond (Eleuthera, Bahamas). Sedimentology 58, 720–738.
Hagadorn, J.W., McDowell, C., 2012. Microbial influence on erosion, grain transport and bedform genesis in sandy substrates under unidirectional flow. Sedimentology 59, 795–808.
Hsu, K.J., Siegenthaler, C., 1969. Preliminary experiments on hydrodynamic movement induced by evaporation and their bearing on the dolomite problem. Sedimentology 12, 11–25.
Iglesias, A., 1981. Temperaturas. In: Chiozza, E., Figueira, R. (Eds.), Atlas Total de la República Argentina. Centro Editor de América Latina, Buenos Aires, pp. 204–208.
Libes, S.M., 1992. An Introduction to Marine Biogeochemistry. John Wiley & Sons, New York (734pp.).
Noffke, N., 2010. Microbial Mats in Sandy Deposits from the Archean Era to Today. Springer-Verlag, Berlin, p. 200.
Noffke, N., Awramik, M., 2013. Stromatolites and MISS—Differences between relatives. GSA Today 23. http://dx.doi.org/10.1130/GSATG187A.1.
Noffke, N., Gerdes, G., Klenke, T., Krumbein, W.E., 2001a. Microbially induced sedimentary structures—a new category within the classification of primary sedimentary structures. Journal of Sedimentary Research 71, 649–656.
Noffke, N., Gerdes, G., Klenke, T., Krumbein, W.E., 2001b. Microbially induced sedimentary structures indicating climatological, hydrological and depositional conditions within Recent and Pleistocene coastal facies zones (southern Tunisia). Facies 44, 23–30.
Noffke, N., Hazen, R., Nhleko, N., 2003. Earth's earliest microbial mats in a siliciclastic marine environment (2.9 Ga Mozaan Group, South Africa). Geology 31, 673–676.
Pan, J., Bournod, C.N., Pizani, N.V., Cuadrado, D.G., Carmona, N.B., 2013a. Characterization of microbial mats from a siliciclastic tidal flat (Bahía Blanca estuary, Argentina). Geomicrobiology Journal 30, 665–674.
Pan, J., Bournod, C.N., Pizani, N.V., Cuadrado, D.G., Vitale, A., Piccolo, M.C., 2013b. Interaction between estuarine microphytobenthos and physical forcings: the role of atmospheric and sedimentary factors. International Journal of Geosciences 4, 352–361.
Paterson, D.M., 1994. Microbiological mediation of sediment structure and behaviour. In: Stal, L.J., Caumette, P. (Eds.), Microbial Mats. Springer-Verlag, Berlin, pp. 97–109.
Porada, H., Bouougri, E., Ghergut, J., 2007. Hydraulic conditions and mat-related structures in tidal flats and coastal sabkhas. In: Schieber, J., Bose, P.J., Eriksson, P.G., Banerjee, S., Sarkar, S., Altermann, W., Catuneanu, O. (Eds.), Atlas of Microbial Mat Features Preserved within the Siliciclastic Rock Record. Elsevier, Amsterdam, pp. 258–265.
Schieber, J., 1999. Microbial mats in terrigenous clastics: the challenge of identification in the rock record. Palaios 14, 3–12.
Schieber, J., 2004. Microbial Mats in the Siliciclastic Rock Record: A Summary of Diagnostic Features. In: Eriksson, P.G., Altermann, W., Nelson, D., Mueller, W.U., Catuneanu, O., Strand, K. (Eds.), The Precambrian Earth: Tempos and Events, Developments in Precambrian Geology. Elsevier, pp. 663–672.
Shinn, E.A., Kendall, C.G.St.C., 2011. Back to the future. The Sedimentary Record 9, 4–9.
Stal, L.J., 2000. Microbial mats and stromatolites. In: Whitton, B.A., Potts, M. (Eds.), The Ecology of Cyanobacteria. Their Diversity in Time and Space. Kluwer Academic, Dordrecht, pp. 61–120.
Stal, L.J., 2010. Microphytobenthos as a biogeomorphological force in intertidal sediment stabilization. Ecological Engineering 36, 236–245.
Stivaletta, N., Barbieri, R., Picard, C., Bosco, M., 2009. Astrobiological significance of the sabkha life and environments of southern Tunisia. Planetary and Space Science 57, 597–605.
Swart, P.K., Oehlert, A.M., Mackenzie, G.J., Eberli, G.P., Reijmer, J.J.G., 2014. The fertilization of the Bahamas by Saharan dust: a trigger for carbonate precipitation? Geology 42, 671–674.
Taher, A.G., Abdel-Motelib, A., 2014. Microbial stabilization of sediments in a recent Salina, Lake Aghormi, Siwa Oasis, Egypt. Facies 60, 45–52.
Tonni, E.P., Cione, A.L., Figini, A.J., 1999. Predominance of arid climates indicated by mammals in the pampas of Argentina during the Late Pleistocene and Holocene. Palaeogeography, Palaeoclimatology, Palaeoecology 147, 257–281.
Warren, J., 2006. Evaporites: Sediments, Resources and Hydrocarbons. Springer, Germany.
Yechieli, Y., Wood, W., 2002. Hydrogeologic processes in saline systems: playas, sabkhas, and saline lakes. Earth-Science Reviews 58, 343–365.